macroscopically removed from the organs and fixed immediately in a solution containing 10% neutral buffered formalin fixative. Serial paraffin sections were cut at 3 μ thick on a microtome and thaw-mounted on glass slides. Tissue sections were stained with hematoxylin and eosin (HE). The granulomatous lesions were classified into three categories on the basis of the inflammatory reaction, as well as the spread of the lesion in the tissue with reference to the tuberculoid granuloma stages and classifications described previously [21,24,25] (Fig. 1). (1) Exudative reaction with epithelioid cells (Figs. 1A and 2A). This represents an early stage of the granuloma formation, characterized by clusters of macrophages and lymphocytes. In some cases, activated macrophages are transformed into epithelioid cells. (2) Proliferative reaction with capsulization (Figs. 1B and 2B). Granulomas are formed as circumscribed lesions. These are characterized by central accumulation of epithelioid cells with a surrounding rim consisting of fibroblasts and lymphocytes. The center of the well-developed granuloma transforms itself into caseous necrosis or calcification.

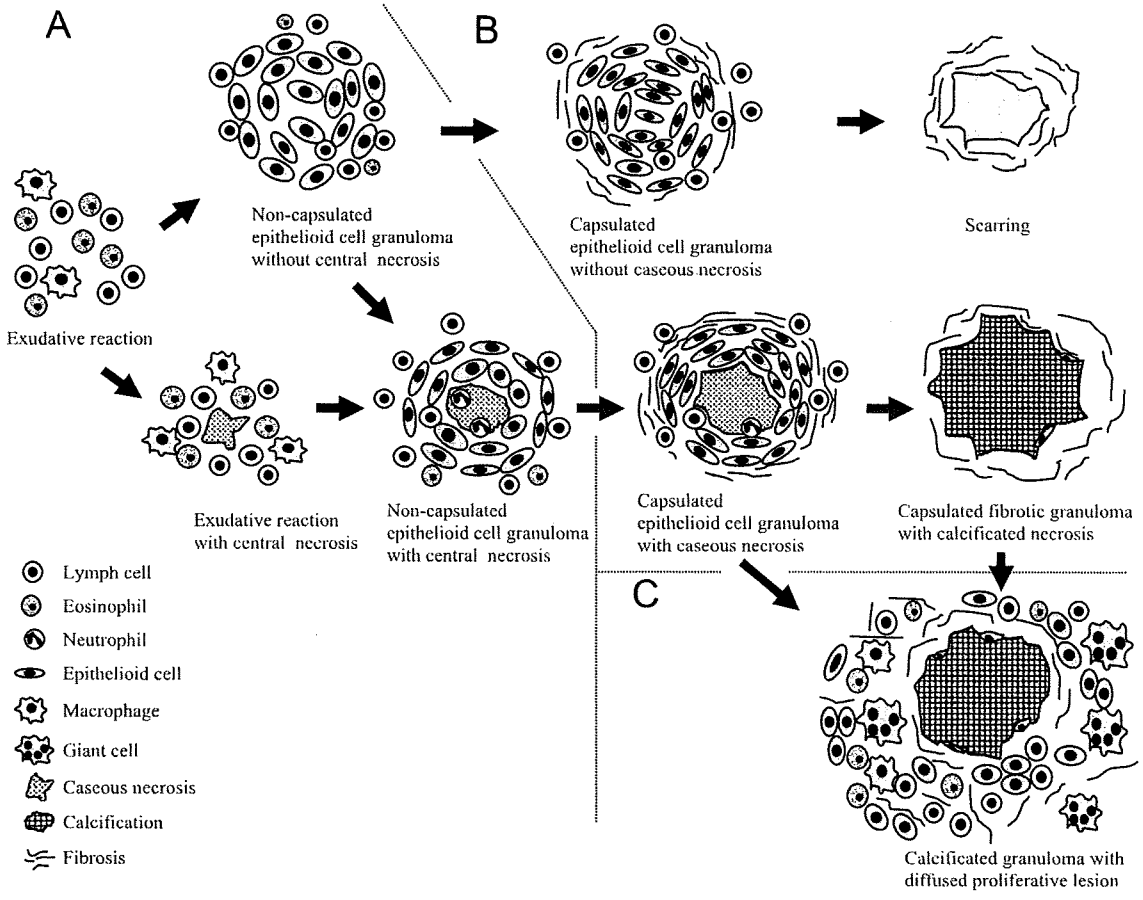

Fig. 1. Schema of pathological changes of *Mycobacterium avium* complex infection in a pig: (A) exudative reaction with epithelioid cells. This represents an early stage of the granuloma formation characterized by clusters of macrophages and lymphocytes. Activated macrophages are transformed into epithelioid cells as granuloma develop. In some cases, the granuloma center causes necrosis without capsulization; (B) proliferative reaction with capsulization. A fibrotic reaction is observed at the rim of the granuloma; and (C) mixed granuloma. In this type of granuloma, an exudative reaction with epithelioid cells is formed around the proliferative reaction with capsulization.

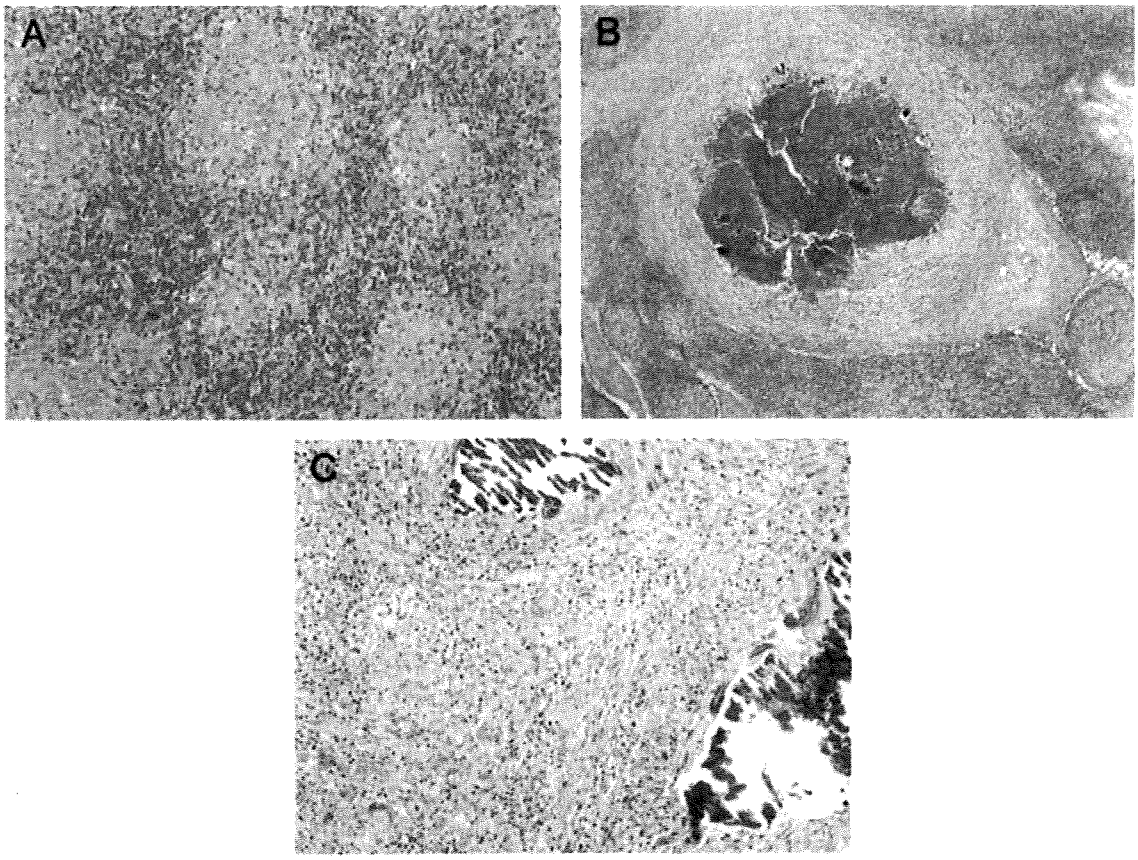

Fig. 2. Histological classification of granulomatous legions in slaughtered pigs: (A) an example of granuloma classified as an exudative reaction with epithelioid cells (mesenteric lymph nodes, HE, × 200). This granuloma has no central necrosis, but infiltration of inflammatory cells (lymphocytes and eosinophils) is observed. Proliferation of macrophages was observed and some of them transformed into epithelioid cells; and (B) an example of granuloma classified as a proliferative reaction with capsulization (mesenteric lymph nodes, HE, × 200). Typical caseous granuloma with central necroses are found surrounded with fibrous capsule. The foci of calcification are also observed in the caseous necroses; and (C) an example of granuloma classified as a mixed granulomas (mesenteric lymph nodes, HE, × 40). Inside the granuloma, extensive proliferations of epithelioid cells, lymphocytes, and fibroblast are observed. Multinucleated giant cells were spreading inside the lesion.

The lesion is distinct from the uninvolved tissues nearby. (3) Mixed granulomas (Figs. 1C and 2C). These are a combination of the exudative reaction with epithelioid cells and the proliferative reaction with capsulization. In some pigs, we found different granuloma stages with in the same tissue section. It was particularly rare to observe a combination of well-developed granuloma and immature granuloma in the same tissue section, and in such cases, we adopted the predominant granuloma pattern for this study.

2.3. Culture examination

After the lesions were collected, the specimens (about 350 mg) were homogenized with ceramic beads in a 1.4 ml carbohydrate solution (TSE kit, Bio-Rad, Paris,

France) using the Multiple-beads Shocker (MB400U, Yasui Kikai, Osaka, Japan), which rapidly cooled them to lower than 5 °C. The homogenized tissues were decontaminated with 2% sodium hydroxide (NaOH) and were centrifuged at 15,000 × *g* for 10 min. The pellets were suspended in 0.1 M phosphate-buffered saline (PBS) (pH 7.4) and inoculated into Ogawa slant medium (Kyokuto Company Limited, Tokyo, Japan) and into the Middlebrook 7H9 medium (Difco, Detroit, MI, USA) with 10% ADC enrichment (Becton, Dickinson and Company, Maryland, USA), followed by incubation for four weeks at 37 °C.

2.4. Identification of isolates

The acid-fast bacilli (AFB) were confirmed using the Fite-Farraco stain method on sliced sections treated according to the methods already mentioned and on a smear of the tissue suspension of an appropriately selected dose.

2.5. Virulence examination

The 11 selected *M. avium*, which were isolated from among the lesions having an exudative reaction with epithelioid cell granulomas ($n = 2$), a proliferative reaction with capsulization ($n = 4$), or the mixed granulomas ($n = 5$), were grown in Middlebrook 7H9 medium to the mid-log phase. The cultured strains were filtered using a 4-μm-pore-size membrane filter (Millipore, Bedford, MA, USA) for dispersal before use. The 11 guinea pigs were infected percutaneously in the lumber portions with an inoculum dose of 10^7 CFU of the strain suspended in 100 μl of PBS. The animal was raised under isolated air condition. The lungs, livers, spleens and kidneys from the guinea pigs were retrieved at seven weeks after infection and prepared for histopathological examination. This experiment was repeated twice using the same strains.

2.6. Isolate genotyping

For MAC DNA typing, restriction fragment length polymorphism (RFLP) was used [26]. Strains were randomly selected from throughout the region during all periods and from all hog farms. The selected 22 isolates from a large collection of the isolated MAC strains were examined by RFLP analysis with insertion sequence IS*1245*, which is representative of a particular MAC strain's mycobacterial pathogenicity [27,28]. Another 30 strains isolated from pigs having limited granulomatous lesions showed the same IS*1245* RFLP pattern in the exploratory experiment. DNA was isolated according to the method described by van Soolingen et al. [26,29]. Approximately 5 μg of purified mycobacterial DNA was digested with restriction endonuclease *Pvu*II (Wako, Osaka, Japan). After separation by electrophoresis in agarose gel, the DNA fragments were exposed to UV in a transilluminator and transferred from the gel to a nylon membrane by vacuum-blot. The DNA was fixed and hybridized with a labeled probe according to the method previously described [29]. The band positions of IS*1245*-containing restriction

fragments were compared with those of a molecular weight marker. The patterns were differentiated according to the number of bands: either "bird type" (three bands) or "non-bird type," (more than three bands) which has been previously described by various authors [30,31].

2.7. Statistical assessment

Elaboration of the data was accomplished using Statview-J5.0 software (Abacus Concept, Inc., Berkeley, CA). Comparison of the groups was done using a paired *t*-test. The χ^2 tests were used to compare categorical variables among groups. $p<0.05$ was considered statistically significant.

3. Results

3.1. Histopathological findings

Granulomatous lesions were found in 986 of the examined 3312 tissues. We classified the mycobacterial lesions into three histopathological categories (Table 1, Fig. 2). Exudative reaction with epithelioid cells was observed in 338 (34.3%) of 986 tissues (Table 1). The appearance of necrosis and fibrosis was observed with a lower prevalence (Table 1, Fig. 2A). The necrosis of this granuloma type was coagulative necrosis. Lymphocytes, eosinophils and giant cells were frequently observed, but neutrophils were rarely observed (Table 1). Most of the giant cells ($n = 135$) were Langhans-type ($n = 50$). Some ($n = 33$) were a foreign-body type with the remaining being of both ($n = 12$). Granulomas that were classified as an exudative reaction with epithelioid cells were predominantly observed in the lung, hepatic and internal iliac lymph nodes (Table 2).

Granulomas classified as a proliferative reaction with capsulization were observed in 500 (50.7%) of 986 tissues from systemically infected slaughtered pigs (Table 1). The appearance of necrosis, calcification and fibrosis was observed with a higher prevalence (Table 1, Fig. 2B). Caseous granulomas were associated with predominant lymphocytes, but also with a few neutrophils and eosinophils (Table 1). Giant cells were relatively rare (Table 1). Langhans-type was observed more than a foreign-body type giant cell (49:5). Granulomas classified as a proliferative reaction with capsulization were predominantly observed in the liver, spleen, mesenteric, pulmonary and superficial lymph nodes (Table 2).

Granulomas classified as a mixed granuloma were observed in 148 (15.0%) of 986 tissues (Table 1). Calcification and fibrosis were observed with a high prevalence, but the fibrosis was formed by irregularly proliferated fibroblasts in diffuse lesions with an accumulation of epithelioid cells (Table 1, Fig. 2C). Lymphocytes, eosinophils, and giant cells were frequently observed in granulomas classified as a mixed granuloma (Table 1). Langhans-type and foreign-body type giant cells were observed (28:22) in about equal measure. Mixed granulomas in each organ were observed with less frequency than the other types of granulomas (Table 2). However, mixed granuloma were observed with comparatively high prevalence in the mesenteric and

Table 1
Difference in stages of progression and cell components for various types of granulomas

Types of granuloma	Total ($n = 986$)	Number (%) having						
		Necrosis	Calcification	Fibrosis	Lymphocytes	Neutrophils	Eosinophils	Giant cells
Exudative reaction with epithelioid cells	338	53 (15.7)	0 (0.0)	41 (12.1)	324 (95.9)	10 (3.0)	170 (50.3)	135 (39.9)
Proliferative reaction with capsulization	500	306 (61.2)	366 (73.2)	489 (97.8)	465 (93.0)	112 (22.4)	115 (23.0)	54 (10.8)
Mixed granuloma	148	66 (44.6)	98 (66.2)	101 (68.2)	148 (100.0)	10 (6.8)	61 (41.2)	85 (57.4)
p-value		<0.0001	<0.0001	<0.0001	NS	<0.0001	<0.0001	<0.0001

NS: not significant ($p<0.05$) for affected tissue obtained from infected pigs ($n = 276$) with MAC.

Table 2
Ratios of various types of granuloma in the organs and lymph nodes of slaughtered pigs

Specimens	Number (%) having:			Total (%)*	*p*-value
	Exudative reaction with epithelioid cells	Proliferative reaction with capsulization	Mixed granuloma		
Organs					
Liver	113 (41.8)	144 (52,7)	16 (5.9)	273 (98.9)	<0.0001
Lung	6 (50.0)	3 (25.0)	3 (25.0)	12 (4.3)	NS
Spleen	10 (46.2)	4 (64.2)	2 (7.7)	16 (5.8)	NS
Kidney	NE	NE	NE	NE	
Lymph nodes					
Mesenteric	28 (10.3)	149 (55.0)	94 (34.7)	271 (98.2)	<0.0001
Hepatic	92 (61.3)	44 (29.3)	14 (9.3)	150 (54.3)	<0.0001
Pulmonary	36 (42.4)	45 (52.9)	4 (4.7)	85 (30.8)	<0.0001
Spleen	3 (75.0)	0 (0.0)	1 (25.0)	4 (1.4)	
Sub-maxillary	31 (26.7)	75 (64.7)	10 (8.6)	116 (42.0)	<0.0001
Superficial cervical	6 (37.5)	9 (56.3)	1 (6.3)	16 (5.8)	NS
Inguinal	9 (24.3)	26 (70.3)	2 (5.4)	37 (13.4)	<0.0001
Internal iliac	2 (66.7)	0 (0.0)	1 (33.3)	3 (1.1)	NS
Sub-iliac	2 (66.7)	1 (33.3)	0 (0.0)	3 (1.1)	NS
Total	338	500	148	986	

NS: not significant ($p<0.05$); and *percentage of total number of examined tissues ($n = 276$) per organs.
NE: not examined.

Table 3
Appearance ratios of acid-fast bacilli among histological types in slaughtered pigs infected with MAC

Organs	Histopathological types			*p*-value
	Exudative reaction with epithelioid cells	Proliferative reaction with capsulization	Mixed granuloma	
Mesenteric lymph nodes	67.9% (19/28)	84.6% (126/149)	78.7% (74/94)	NS
Liver	35.4% (40/113)	34.7% (50/144)	31.3% (5/16)	NS

Figures in parentheses indicate the number of tissues with acid-fast bacilli in relation to the total number for each histological type. NS: not significant ($p<0.05$).

internal iliac lymph nodes (Table 2). In most granulomas with extensive caseous necrosis, a fibrotic reaction replacing the epithelioid cell layer was observed (Fig. 2C).

Eosinophils appeared during any of the granuloma stages, but were frequently observed in granuloma classified as an exudative reaction with epithelioid cells.

There was paucibacillary observation of AFB in all granuloma types (data not shown). The appearance ratios of AFB on mesenteric lymph nodes were 67.9% for the exudative reaction with epithelioid cells, 84.6% for the proliferative reaction with capsulization and 78.7% for the mixed granuloma (Table 3). Histopathological types and bacterial load were not correlated (Table 3).

When the occurrence of AFB was compared according to the criterion of whether or not giant cells exist in the lesions independent of the histopathological type, no significant difference was found in either the mesenteric lymph nodes or the liver (Table 4).

3.2. Distribution of granulomatous lesions across organs

The granulomatous lesions were found almost exclusively in the liver and mesenteric lymph nodes (Table 2). Lesions in sub-iliac and internal-iliac lymph nodes showed the lowest prevalence (Table 2).

Lesions in the liver were concentrated in the portal area with a few exceptions, and they occasionally caused invasive necrosis for the contiguous hepatic lobule (Fig. 5B).

3.3. Comparison of types of granuloma on each organ

When the types of granulomas were compared between mesenteric lymph nodes and liver for systemically infected cases ($n = 209$), the exudative reaction with epithelioid cells and the proliferative reaction with capsulization showed comparatively the same histological types, but differences were observed among the mixed granulomas (Fig. 3). Individuals with mixed granulomas in mesenteric lymph nodes showed different histological types in the liver (Fig. 3).

Furthermore, we examined the histological types for cases having lesions across the mesenteric lymph nodes, liver, and superficial lymph nodes ($n = 46$). An individual with exudative reaction with epithelioid cells in the mesenteric lymph nodes and liver showed a proliferative reaction with capsulization in superficial

Table 4
Appearance ratios of acid-fast bacilli attributable to giant cells in slaughtered pigs infected with MAC

Organs	Existence of giant cell		*p*-Value
	No giant cell	Existence of giant cell	
Mesenteric lymph nodes	86.1% (161/187)	69.0% (58/84)	NS
Liver	34.4% (74/215)	36.2% (21/58)	NS

Figures in parentheses indicate the number of tissues with acid-fast bacilli in relation to the total number with or without giant cells in each organ. NS: not significant ($p > 0.05$).

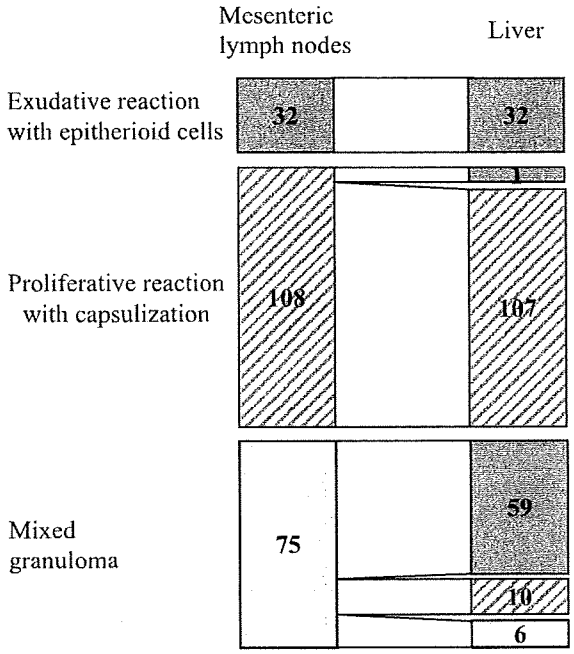

Fig. 3. Comparison of the granuloma types for mesenteric lymph nodes and livers in individuals. Each individual showed a relatively identical granuloma type resulting in the mesenteric lymph nodes as well as in the liver. However, some pigs with mixed granulomas in mesenteric lymph nodes showed different granuloma types in the liver.

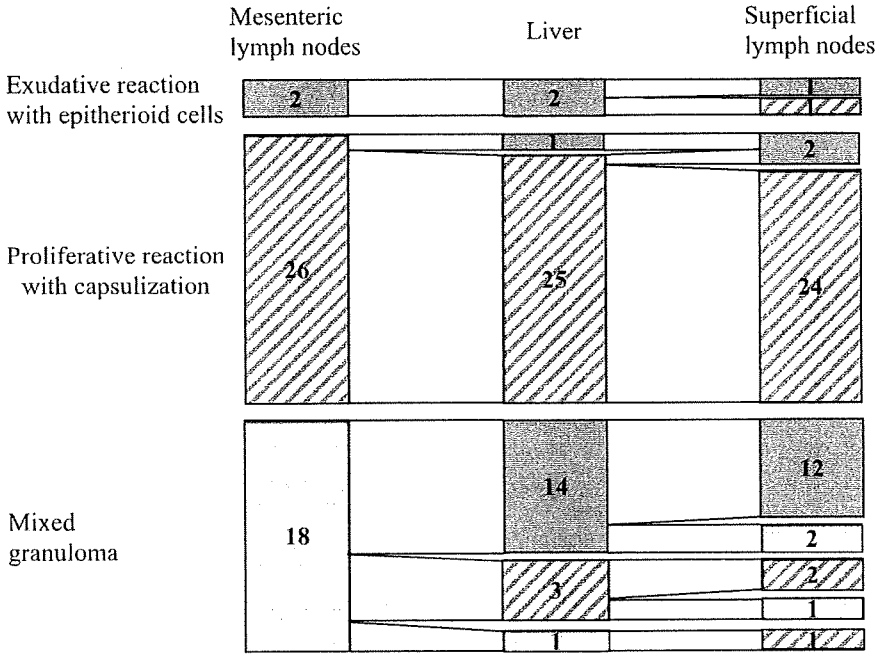

Fig. 4. Comparison of the types of granulomas in the mesenteric lymph nodes, liver, and superficial lymph nodes of individual pigs. Each individual showed relatively identical granuloma types among the various organs. However, some individuals showed different granuloma types among the various organs. There was a relatively higher ratio for individuals with mixed granuloma in the mesenteric lymph nodes.

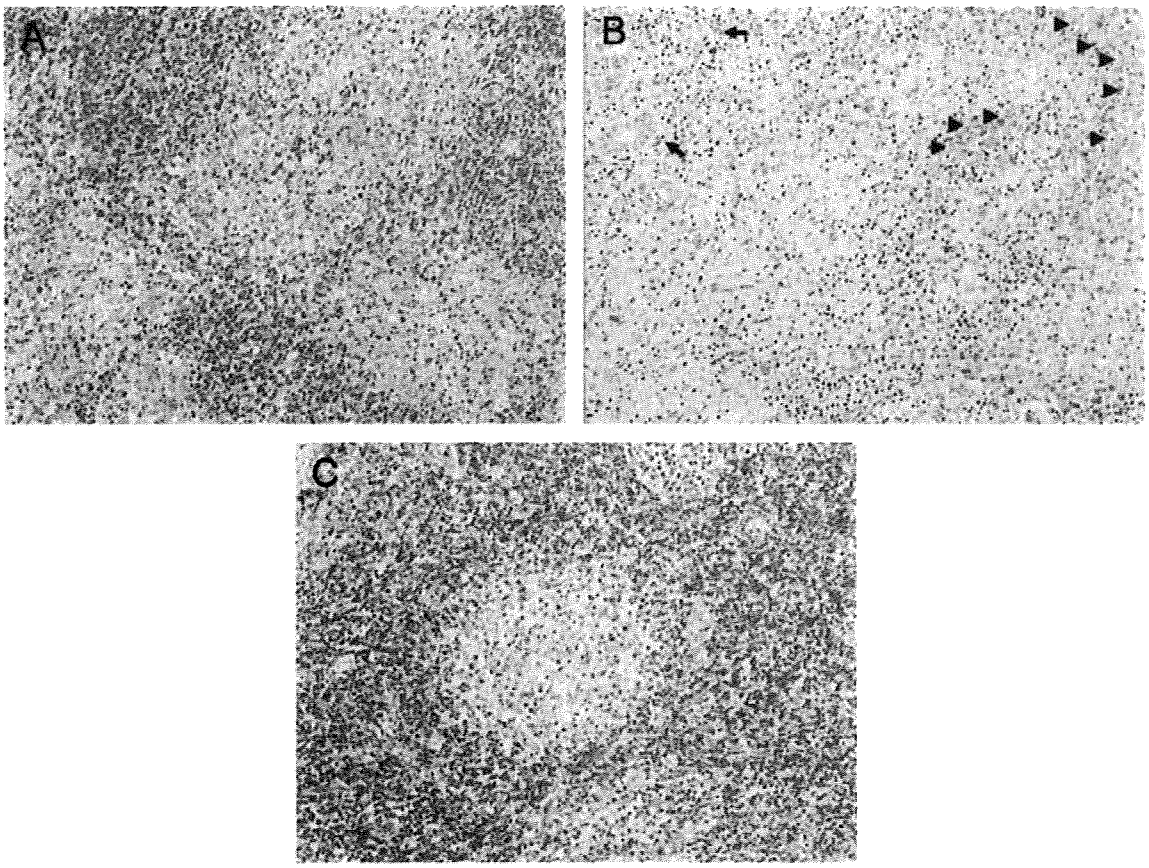

Fig. 5. Exudative reaction with epithelioid cells in a systemically infected pig: (A) a diffuse granulomatous lesion with moderate eosinophils and macrophages observed in the mesenteric lymph node (HE, × 200). A growing epithelioid cell granuloma was observed; (B) an exudative lesion with macrophage, lymphocytes and eosinophils observed in the portal area of the liver (HE, × 200). The lesion invaded the contiguous hepatic lobule, and the remaining hepatic cords were confirmed (arrow heads). Arrows indicate an interlobular bile duct; and (C) a focal accumulation of epithelioid cells with lymphocytes and eosinophils observed in the inguinal lymph node (HE, × 200).

lymph nodes (Fig. 4). Granuloma types of lesions among mesenteric lymph nodes, liver and superficial lymph nodes were almost the same with regard to the proliferative reaction with capsulization (Fig. 4). Individuals with mixed granulomas on mesenteric lymph nodes showed different histological types in the liver and superficial lymph nodes (Fig. 4). Figs. 5–7 show examples of each case that resulted in granuloma across the mesenteric lymph node, liver, and superficial lymph nodes in a systemically infected pig.

3.4. Experimental infection

All infected lesions showed microgranulomas without caseous necrosis in the guinea pigs (Fig. 8A–C). The component cells of the granulomas were epithelioid cells and lymphocytes. There were no significant differences concerning distribution of the lesions in the reproducibility of pig's histological features.

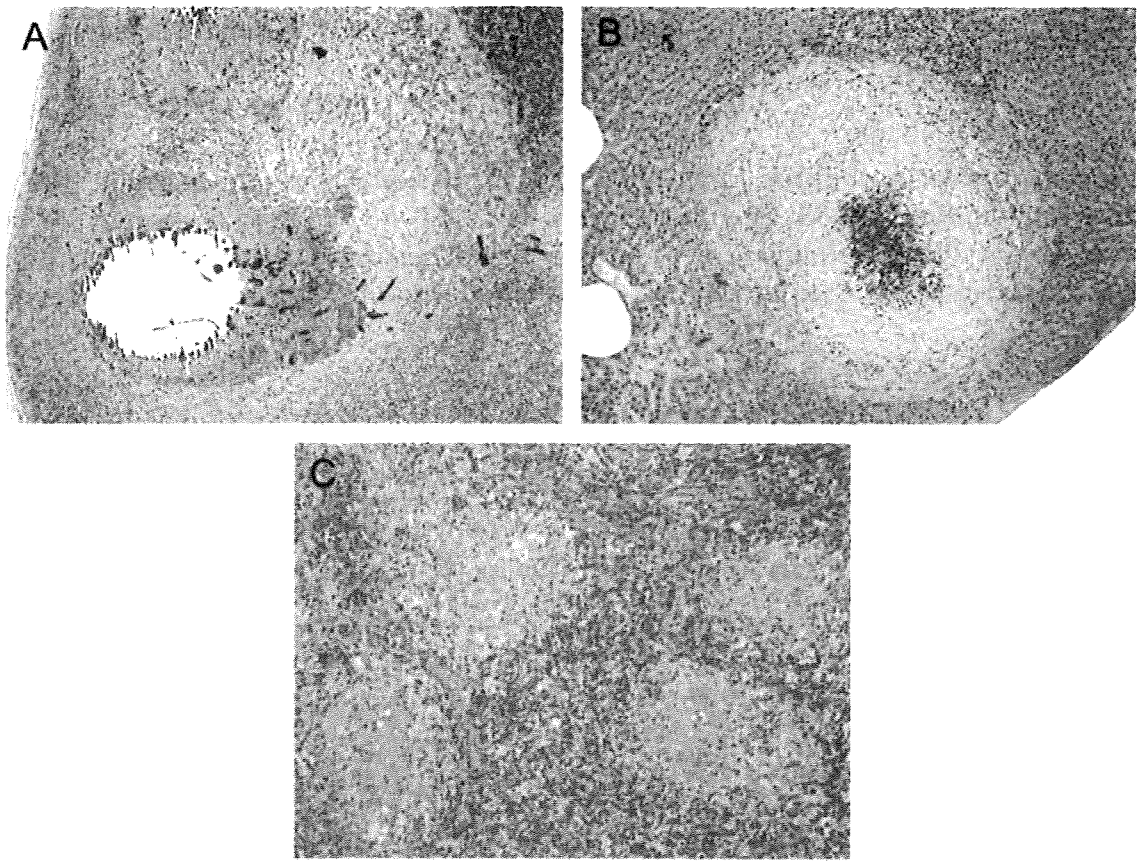

Fig. 6. Proliferative reaction with capsulization in a systemically infected pig: (A) granuloma with caseous necrosis with calcification observed in the mesenteric lymph node (HE, × 100); (B) well-capsulated granulomas with early central caseation observed under hepatic capsule in the liver (HE, × 100); and (C) early active epithelioid cell granuloma observed in the inguinal lymph nodes (HE, × 100).

This experiment was repeated twice using the same strains, and the same results were obtained.

3.5. *Gene analysis of strain with* IS *1245 RFLP*

Isolates were obtained from 33 hog farms on the Okinawa islands. All the isolated strains were also distinguished between *Mycobacterium avium* (*M. avium*) and other sub-species by the multiplex PCR method [32]. All strains possessed IS *1245* in their genes. IS *1245* RFLP analysis was divided into two homogenous types: Type I was characterized with homogenous six bands and Type II was characterized with mostly identical multi-bands >20. However, the "bird-type" with three bands was not observed (Fig. 9). The breakdown by genotype and histological characteristics was as follows: for the strain group with type I, exudative reaction with epithelioid cells ($n = 0$), proliferative reaction with capsulization ($n = 2$), and mixed granulomas ($n = 3$); and for the strain group with type II, and exudative reaction with epithelioid cells ($n = 3$), proliferative reaction with capsulization ($n = 8$), and mixed

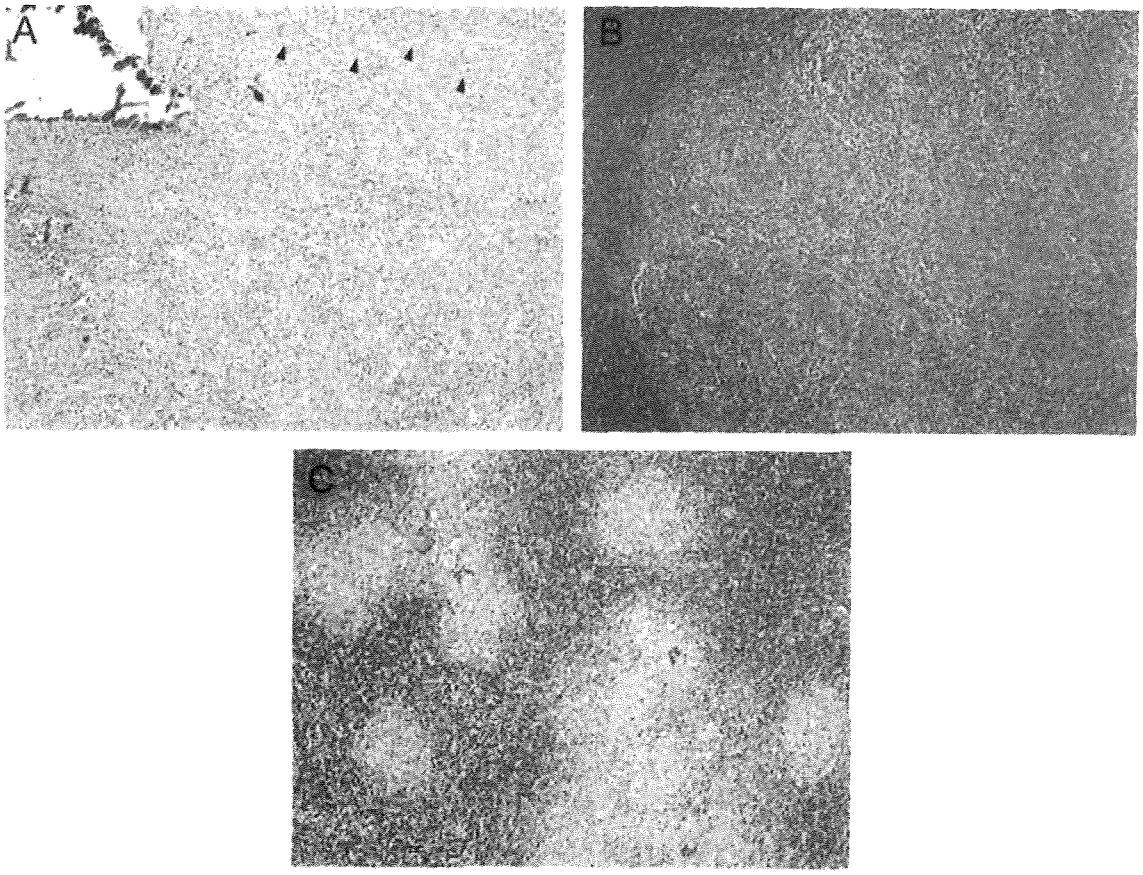

Fig. 7. Mixed granulomas in a systemically infected pig: (A) a mixed granuloma lesion shows a calcified granuloma coexisting with diffuse inflammatory lesions consisting of numerous lymphoid cells and macrophages, Langhans-type giant cells (arrow heads) in mesenteric lymph nodes (HE, × 40); (B) many multifocal epithelioid cell granulomas with severe lymphocyte inflammation observed in the portal area of the liver (HE, × 40); and (C) epithelioid cell granulomas observed focally in the inguinal lymph node (HE, × 40).

granuloma ($n = 8$). A few bands were common between types I (D, E) and II (A, B, C) (Fig. 9A–E).

4. Discussion

The present study indicated that pigs showed a variety of histological pictures from exudative to fibrotic reactions caused by MAC infection. It is common knowledge that in human tuberculosis, epithelioid cell granuloma changes to caseous granuloma with the development of granuloma [24]. Acland et al. examined the sequential morphological changes in orally inoculated pigs and showed that the picture changes from accumulated initial lesion of epithelioid cells to well-capsulated calcificated granuloma [22]. Thus, it may be possible to explain the histological differences of granulomas according to a difference in the phase of infection. Although this might be the main reason that there were a variety of granulomas, it is very difficult to evaluate differences in the phases of infection with spontaneously

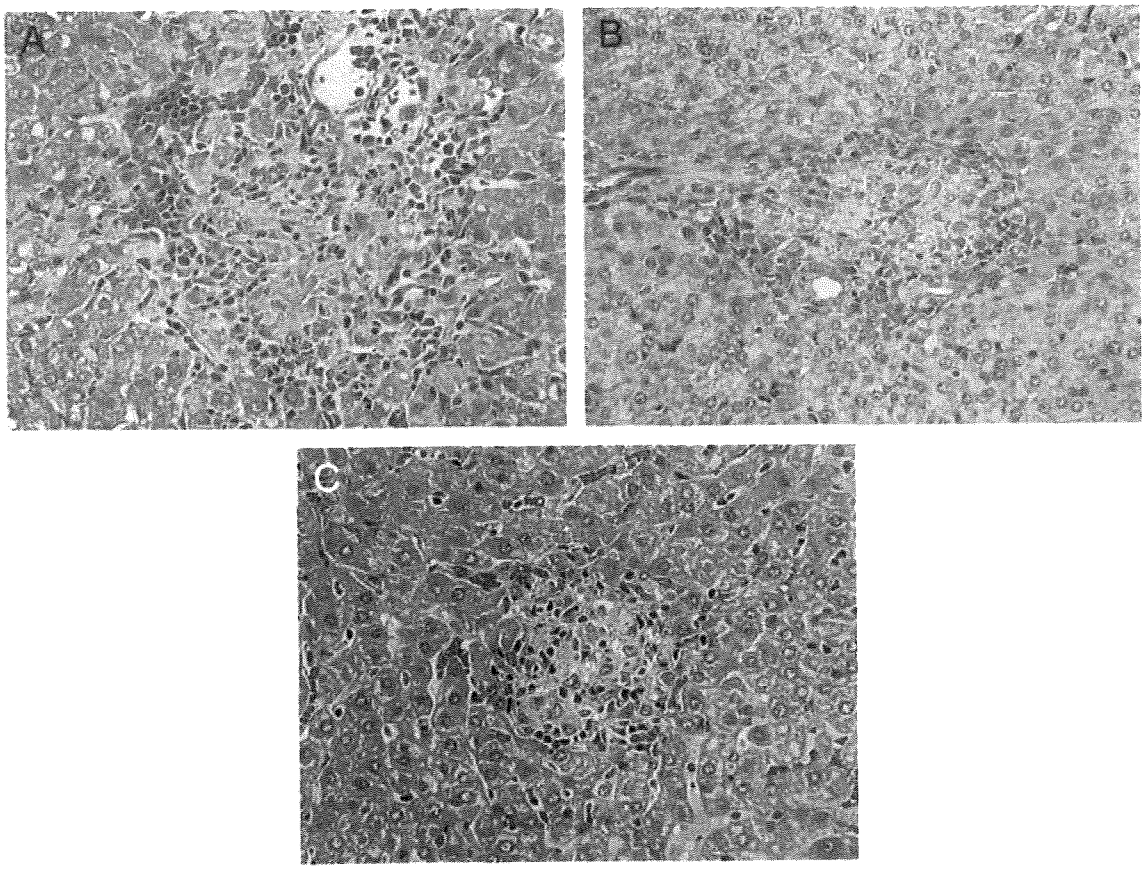

Fig. 8. Histological findings of guinea pigs inoculated with strains that showed different granuloma types in slaughtered pigs. Micro-epithelioid cell granulomas were observed in the livers of all guinea pigs: (A) the liver of a guinea pig inoculated with the strain that showed an exudative reaction with epithelioid cells in pigs (HE, × 200); (B) the liver of guinea pig inoculated with the strain that showed a proliferative reaction with capsulization in pigs (HE, × 200); and (C) the liver of the guinea pig inoculated with the strains that showed the mixed granuloma in pigs (HE, × 200).

infected cases. There are two other possibilities for the cause of the different types of granuloma: bacterial factors and host factors. However, RFLP IS*1245* patterns did not correlate with certain granuloma types in this study. In addition, the most prevalent serotype of the strains isolated from the affected tissue was type 4 (unpublished data). Furthermore, most strains with the same genotype showed pathogenicity for guinea pigs irrespective of the granuloma type. These findings may suggest that bacterial factors did not play a major role in the formation of different types of granuloma. Since we did not assess host immunological status in the present study, this issue needs to be discussed in further immunological research regarding MAC infection in pigs. However, Iwakiri et al. indicated that disseminatedly infected pigs showed a strong reaction to purified protein derived (PPD) from *M. avium* when compared to the lymphoproliferative response between localized infected pigs and disseminatedly infected pigs [33]. Ellsworth et al. also showed the same result in a disseminatedly infected sow [23]. This may suggest that cell-mediated immunity is maintained in systemically infected pigs. The effects of viral infection should also be

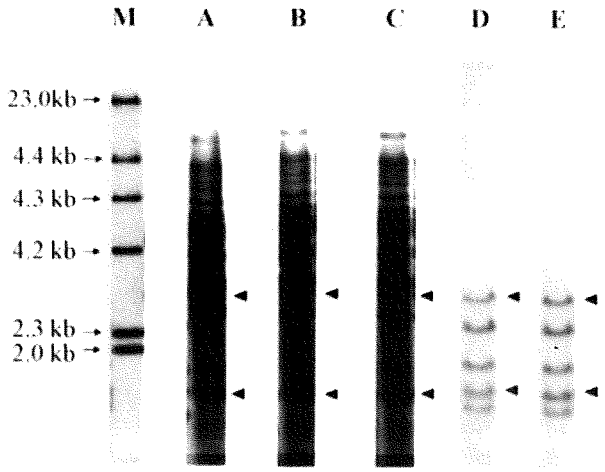

Fig. 9. IS *1245* RFLP type of strains showed different histological types in slaughtered pigs: (A) a genomic pattern in a strain isolated from a proliferative reaction with capsulization; (B) a strain showing an exudative reaction with epithelioid cells showed the same genomic pattern as A; (C) a strain from a mixed granuloma showed the same result; (D) a genomic pattern with six bands was revealed in a strain which showed a proliferative reaction with capsulization; and (E) a strain that appeared as a mixed granuloma showed the same result. *M* is the molecular weight marker. Arrow heads indicate a few common bands that were observed between the group of (A), (B), (C), and the group of (D), (E).

considered because porcine circo virus or porcine reproductive and respiratory syndrome virus affect the immunity of a pig [34–36].

In the present study, we observed the accumulation of eosinophils through a variety of granulomatous lesions. Recent work has suggested a mycobacterial effect of peroxidase in eosinophilial granules [37]. However, it is unknown whether the infiltration is specific to MAC infection because eosinophils are observed more frequently in pigs than in other species. Additionally, infiltrations of eosinophils in granulomatous lesions were not observed in the guinea pig inoculated strains isolated from the pigs. However, Castro et al. showed that heat-killed mycobacteria cause rapid chemotaxis in a large number of eosinophils in mice [38]. Therefore, the role of eosinophils in MAC granuloma should be studied in further research.

It has been reported that giant cells are observed more frequently in granuloma without caseation necrosis than granuloma with caseation necrosis in human MAC disease [39]. This finding is consistent with our present findings that giant cells were observed more frequently in an immature granuloma. The appearance of giant cells was recognized between 6 and 12 weeks after inoculation of *M. avium* in pigs [22], and well-developed granulomas were formed at 12 weeks after oral infection in mesenteric lymph nodes [21]. Because most of the pigs that we used in this study were about 6 months old, these findings may indicate that giant cells are dominant at an earlier granuloma stage.

In the present study, we frequently observed a proliferative reaction with calcification. Some previous researchers have also observed calcificated granuloma in spontaneously affected pigs [20,23]. Experimentally, calcification was shown in more advanced granuloma in pigs scarified at 12 weeks after inoculation [21]. These

findings may suggest that calcification frequently occurs at about 3 months after infection in the pig. In human MAC disease, calcification of caseous necrosis is rare [40] and in a previous review of tuberculosis, the appearance of calcification may require at least one or two years [41]. However, it is very difficult to evaluate the difference in phases and frequency of calcification between pigs and humans.

In pigs, the development of localized lesions in lymph nodes of the digestive tract are usually observed [42]. Windsor et al. showed that lesions commonly appearing in the liver and mesenteric lymph nodes in systemically infected pigs [15]. We observed the same results in the present study and most lesions in the liver were localized in the hepatic portal area. Ellsworth et al. have proved that granulomatous lesions in intestinal organs are caused by oral infection of MAC [43]. Such evidence suggests the gastrointestinal tract as the most likely route of MAC infection, with the respiratory tract as a less frequent pathway in pigs. In addition, although granulomatous lesions are frequently observed in the draining lymph nodes in pigs MAC infection, it is uncommon in human respiratory MAC infection [7,44].

In the present study, a histopathological response was maintained among the organs in systemically infected pigs, but most mixed granuloma showed more immature granuloma in the liver and superficial lymph nodes. Savov and Pavlov showed that the existence of histopathological changes in the lymph nodes had a proliferative to infiltrative character [20]. In addition, thorough histological examination of an aborted sow, they also demonstrated diffuse and focal non-encapsulated granulomas in lymph nodes and parenchymatous organs, and a few encapsulated calcified foci in the endometrium [23]. Farhi et al. have reported histopathological findings in disseminated human cases of immunosuppressed and immunocompetent hosts; and they have demonstrated that tuberculoid granulomas are observed in the liver and spleen, and that a variety of non-necrotizing and necrotizing granulomatous lesions are observed in lymph nodes [11]. These findings support the possibility that the histological futures change across organs in systematically infected host.

Previous studies of systemic mycobacteriosis reported that diffuse lesions are multibacillary, but localized lesions are paucibacillary in an immunocompromised host [1,12]. These findings differ from our present results with domestic pigs in that the exudative reaction with epithelioid cells showed paucibacillary lesions. Nakamura et al. also showed that only a small number of AFB was observed histologically in pigs dosed with MAC [21]. This discrepancy between systemic infection of pigs and systemic infection of humans may be attributed to the immunity of host, and should be clarified it in further investigation.

Our investigation revealed that there are some differences in the histopathological features of pig MAC infection from those of human pulmonary MAC infection [4,7,40]: (1) eosinophils appear with relatively high frequency in immature granuloma; (2) possibility of oral infection; (3) organisms caused dissemination in pigs and show different patterns of granulomatous lesions; and (4) pigs about 6 months old in contrast to that calcification is very rare in human MAC infection.

Acknowledgments

We would like to acknowledge the contribution made by inspectors working at slaughter houses in Okinawa Prefecture for their assistance in the gross examination and collection of samples.

References

[1] Inderlied CB, Kemper CA, Bermudez LE. The *Mycobacterium avium* complex. Clin Microbiol Rev 1993;6:266–310.
[2] Prince DS, Peterson DD, Steiner RM, Gottlieb JE, Scott R, Israel HL, et al. Infection with *Mycobacterium avium* complex in patients without predisposing conditions. N Engl J Med 1989; 321:863–8.
[3] Kurashima A. Clinical study on development of nontuberculous mycobacterial lung disease. Kekkaku 2004;79:737–41.
[4] Fujita J, Ohtsuki Y, Suemitsu I, Shigeto E, Yamadori I, Obayashi Y, et al. Pathological and radiological changes in resected lung specimens in *Mycobacterium avium intracellulare* complex disease. Eur Respir J 1999;13:535–40.
[5] Ridley DS. Histopathological classification and the immunological spectrum of the leprosy. Bull World Health Organ 1974;151:451–65.
[6] Ridley DS, Ridley MJ. Rationale for the histological spectrum of tuberculosis. A basis for classification. Pathology 1987;19:186–92.
[7] Fujita J, Ohtsuki Y, Shigeto E, Suemitsu I, Yamadori I, Bandoh S, et al. Pathological findings of bronchiectases caused by *Mycobacterium avium intracellulare* complex. Respir Med 2003;97: 933–8.
[8] Zakowski P, Fligiel S, Berlin GW, Johnson Jr L. Disseminated *Mycobacterium avium-intracellulare* infection in homosexual men dying of acquired immunodeficiency. JAMA 1982;248:2980–2.
[9] Greene JB, Sidhu GS, Lewin S, Levine JF, Masur H, Simberkoff MS, et al. *Mycobacterium avium-intracellulare*: a cause of disseminated life-threatening infection in homosexuals and drug abusers. Ann Intern Med 1982;97:539–46.
[10] Sohn CC, Schroff RW, Kliewer KE, Lebel DM, Fligiel S. Disseminated *Mycobacterium avium-intracellulare* infection in homosexual men with acquired cell-mediated immunodeficiency: a histologic and immunologic study of two cases. Am J Clin Pathol 1983;79:247–52.
[11] Farhi DC, Mason 3rd. UG, Horsburgh Jr CR. Pathologic findings in disseminated *Mycobacterium avium-intracellulare* infection. A report of 11 cases. Am J Clin Pathol 1986;85:67–72.
[12] Klatt EC, Jensen DF, Meyer PR. Pathology of *Mycobacterium avium-intracellulare* infection in acquired immunodeficiency syndrome. Hum Pathol 1987;18:709–14.
[13] Okumura M, Iwai K, Ogata H, Mizutani S, Yoshimori K, Itoh K, et al. Pulmonary *Mycobacterium avium* complex disease showing nodular bronchiectasis: pathological findings in two cases. Kekkaku 2002;77:717–23.
[14] Songer JG, Bicknell EJ, Thoen CO. Epidemiological investigation of swine tuberculosis in Arizona. Can J Comp Med 1980;44:115–20.
[15] Windsor RS, Durrant DS, Burn KJ, Blackburn JT, Duncan W. Avian tuberculosis in pigs: miliary lesions in bacon pigs. J Hyg (London) 1984;92:129–38.
[16] Gardner IA, Hird DW. Environmental source of mycobacteriosis in a California swine herd. Can J Vet Res 1989;53:33–7.
[17] Morita Y, Maruyama S, Katsube Y. Prevalence of atypical mycobacteriosis in slaughtered swine in Gunma Prefecture and the serovars of the isolates. J Vet Med Sci 1994;56:475–9.
[18] Matlova L, Dvorska L, Palecek K, Maurenc L, Bartos M, Pavlik I. Impact of sawdust and wood shavings in bedding on pig tuberculosis lesions in lymph nodes, and IS*1245* RFLP analysis of *Mycobacterium avium subsp. hominissuis* of serotypes 6 and 8 isolated from pigs and environment. Vet Microbiol 2004;102:227–36.

[19] Tanaka H, Kobayashi EJ. Education and research using experimental pigs in a medical school. Artif Organs 2006;9:136–43.
[20] Savov N, Pavlov N. Swine infected with atypical mycobacteria. Vet Med Nauki 1976;13:83–90.
[21] Nakamura K, Yokomizo Y, Okutomo M, Nishimori K, Yugi H, Shoya S. Light and electron microscopic observations on granulomatous lesions in pigs dosed with *Mycobacterium intracellulare*. J Comp Pathol 1984;94:509–19.
[22] Acland HM, Whitlock RH. *Mycobacterium avium* serotype 4 infection of swine: the attempted transmission by contact and the sequence of morphological changes in inoculated pigs. J Comp Pathol 1986;96:247–66.
[23] Ellsworth SR, Kirkbride CA, Johnson DD, Vorhies MW. *Mycobacterium avium* abortion in a sow. Vet Pathol 1979;16:310–7.
[24] Huebschmann P. Pathological anatomie der tuberkulose. Heidelberg: Julius Springer; 1928.
[25] Corpa JM, Garrido J, Garcia Marin JF, Perez V. Classification of lesions observed in natural cases of paratuberculosis in goats. J Comp Pathol 2000;122:255–65.
[26] van Soolingen D, Bauer J, Ritacco V, Leao SC, Pavlik I, Vincent V, et al. IS*1245* restriction fragment length polymorphism typing of *Mycobacterium avium* isolates: proposal for standardization. J Clin Microbiol 1998;36:3051–4.
[27] Kunze ZM, Wall S, Appelberg R, Silva MT, Portaels F, McFadden JJ. IS*901*, a new member of a widespread class of atypical insertion sequences, is associated with pathogenicity in *Mycobacterium avium*. Mol Microbiol 1991;5:2265–72.
[28] Guerrero C, Bernasconi C, Burki D, Bodmer T, Telenti A. A novel insertion element from *Mycobacterium avium*, IS*1245*, is a specific target for analysis of strain relatedness. J Clin Microbiol 1995;33:304–7.
[29] Meyer M, von Grunberg PW, Knoop T, Hartmann P, Plum G. The macrophage-induced gene mig as a marker for clinical pathogenicity and in vitro virulence of *Mycobacterium avium* complex strains. Infect Immun 1998;66:4549–52.
[30] Ritacco V, Kremer K, van der Laan T, Pijnenburg JE, de Haas PE, van Soolingen D. Use of IS*901* and IS*1245* in RFLP typing of *Mycobacterium avium* complex: relatedness among serovar reference strains, human and animal isolates. Int J Tuberc Lung Dis 1998;2:242–51.
[31] Oliveira RS, Sircili MP, Oliveira EM, Balian SC, Ferreira-Neto JS, Leao SC. Identification of *Mycobacterium avium* genotypes with distinctive traits by combination of IS*1245*-based restriction fragment length polymorphism and restriction analysis of hsp65. J Clin Microbiol 2003;41:44–9.
[32] Iwakiri A, Sedoyama T, Saito H, Toshimasu M, Goto Y, Shinjo T. Mycobacteria species isolated from swine bred in southern Kyushu area. J Jpn Vet Med Assoc 1999;52:663–6.
[33] Iwakiri A, Toshimasu M, Xu DL, Shinjo T, Goto Y. Lymphoproliferative responses in pigs infected with *Mycobacterium avium*. J Vet Med Sci 2001;63:827–9.
[34] Kawashima K, Tsunemitsu H, Horino R, Katsuda K, Onodera T, et al. Effects of dexamethasone on the pathogenesis of porcine circovirus type 2 infection in piglets. J Comp Pathol 2003;129:294–302.
[35] Murtaugh MP, Xiao Z, Zuckermann F. Immunological responses of swine to porcine reproductive and respiratory syndrome virus infection. Viral Immunol 2002;15:533–47.
[36] Xiao Z, Batista L, Dee S, Halbur P, Murtaugh MP. The level of virus-specific T-cell and macrophage recruitment in porcine reproductive and respiratory syndrome virus infection in pigs is independent of virus load. J Virol 2004;78:5923–33.
[37] Borelli V, Vita F, Shankar S, Soranzo MR, Banfi E, Scialino G, et al. Human eosinophil peroxidase induces surface alteration, killing, and lysis of *Mycobacterium tuberculosis*. Infect Immun 2003;71:605–13.
[38] Castro AG, Esaguy N, Macedo PM, et al. Live but not heat-killed mycobacteria cause rapid chemotaxis of large numbers of eosinophils in vivo and are ingested by the attracted granulocytes. Infect Immun 1991;59:3009–14.
[39] Fujita J, Ohtsuki Y, Suemitsu I, Yamadori I, Shigeto E, Shiode M, et al. Immunohistochemical distribution of epithelioid cell, myofibroblast, and transforming growth factor-beta1 in the granuloma caused by *Mycobacterium avium intracellulare* complex pulmonary infection. Microbiol Immunol 2002;46:67–74.

[40] Kobashi Y, Fukuda M, Yoshida K, Miyashita N, Niki Y, Oka M. Four cases of pulmonary *Mycobacterium avium intracellulare* complex presenting as a solitary pulmonary nodule and a review of other cases in Japan. Respirology 2006;11:317–21.
[41] Corrin B. Pathology of the lung. UK: Churchill Livingstone; 2000. p. 177–92.
[42] Thorel MF, Huchzermeyer H, Weiss R, Fontaine JJ. *Mycobacterium avium* infections in animals. Vet Res 1997;28:439–47.
[43] Ellsworth S, Kirkbride CA, Johnson DD. Excretion of *Mycobacaterium avium* from lesions in the intestine and tonsils of infected swine. Am J Vet Res 1980;41:1526–30.
[44] Moore EH. Atypical mycobacterial infection in the lung: CT appearance. Radiology 1993;187: 777–82.

THE JOURNAL OF BIOLOGICAL CHEMISTRY VOL. 282, NO. 51, pp. 36923–36932, December 21, 2007

Gp120 V3-dependent Impairment of R5 HIV-1 Infectivity Due to Virion-incorporated CCR5*

Received for publication, June 28, 2007, and in revised form, October 11, 2007 Published, JBC Papers in Press, October 30, 2007, DOI 10.1074/jbc.M705298200

Kazuaki Monde‡, Yosuke Maeda‡, Yuetsu Tanaka§, Shinji Harada‡, and Keisuke Yusa‡1

From the ‡Department of Medical Virology, Graduate School of Medical Sciences, Kumamoto University, Honjo 1-1-1, Kumamoto 860-8556, Japan and the §Department of Infectious Disease and Immunology, Okinawa-Asia Research Center of Medical Science, Faculty of Medicine, University of the Ryukyus, Uehara 207, Nishihara, Okinawa 903-0215, Japan

Entry of R5 human immunodeficiency virus type 1 (HIV-1) into target cells requires sequential interactions of the envelope glycoprotein gp120 with the receptor CD4 and the coreceptor CCR5. We investigated replication of 45 R5 viral clones derived from the HIV-$1_{JR\text{-}FLan}$ library carrying 0–10 random amino acid substitutions in the gp120 V3 loop. It was found that 6.7% (3/45) of the viruses revealed ≥10-fold replication suppression in PM1/CCR5 cells expressing high levels of CCR5 compared with PM1 cells expressing low levels of CCR5. In HIV-$1_{V3L\#08}$, suppression of replication was not associated with entry events and viral production but with a marked decrease in infectivity of nascent progeny virus. HIV-$1_{V3L\#08}$, generated from infected PM1/CCR5 cells, was 98% immunoprecipitated by anti-CCR5 monoclonal antibody T21/8, whereas the other infectious viruses were only partially precipitated, suggesting that incorporation of larger amounts of CCR5 into the virions caused impairment of viral infectivity in HIV-$1_{V3L\#08}$. The results demonstrate the implications of an alternative influence of CCR5 on HIV-1 replication.

Entry of R5 human immunodeficiency virus type 1 (HIV-1)[2] into a target cell requires cooperative interactions of the viral envelope protein gp120 with the receptor CD4 and the coreceptor CCR5 (or CXCR4 for X4 HIV-1) (1–3). These interactions depend on the concentration and distribution of receptor and coreceptor molecules on the cell surface (4–7). Cells with a large amount of CD4 only require trace amounts of CCR5 for maximal susceptibility to infection by R5 HIV-1, whereas cells low in CD4 require larger amounts of CCR5 for maximal infection (6, 8). Sequential binding of the viral surface glycoprotein gp120 to CD4 and CCR5 initiates R5 HIV-1 infection; CD4 attachment induces a conformational change in gp120 that exposes a CCR5 binding domain (9–11). The coreceptor-binding site located in the bridging sheet and the V3 loop of gp120 also play a crucial role in interacting with the N-terminal domains of the CCR5 (12–16). Finally, direct interaction between CCR5 and the V3 loop (35–37 amino acid residues) in gp120 induces structural rearrangements of a fusion peptide of gp41, allowing fusion of viral and cellular membranes (14, 15, 17–19).

Envelope viruses are known to down-modulate the receptor expression on infected cells to prevent reinfection (20, 21). Post-entry, HIV infection leads to a rapid and potent down-modulation of CD4 molecules expressed at the cell surface. Three viral gene products, Nef, Env, and Vpu, are involved in trafficking and catabolism of down-modulating CD4. Nef enhances CD4 internalization and directs the receptor to lysosomes for degradation (22–27), whereas Env and Vpu interfere with the transport of newly synthesized CD4 to the cell surface (28, 29). Without strict CD4 down-modulation, CD4 induces trapping and aggregation of nascent progeny virions at the cell surface by the high affinity of gp120 for CD4 (30) and a dramatic reduction in the infectivity of released virions by recruitment and sequestration of gp120 molecules away from budding sites or recruitment of nonfunctional gp120-CD4 complexes at the virion surface (31, 32).

On the other hand, strict down-modulation of coreceptor CCR5 is not observed in HIV-infected cells, although CCR5 expression on the cell surface is partially reduced by Nef (33). Partial down-regulation of CCR5 and strict down-regulation of CD4 prevent the superinfection of cells in which viral replication is already progressing. CCR5 binding domains, V3 loop, and the bridging sheet domain of gp120 are not exposed until conformational changes in gp120 are induced by interaction with CD4 on the cell surface; therefore, CCR5 would not trap nascent progeny virions at the cell surface. This may be one reason why CCR5 does not need to be strictly down-regulated after viral entry. However, a presence of an unknown inhibitory effect of CCR5 on R5 HIV-1 replication is possible. This paper addresses whether the level of CCR5 in CD4 T-cell lines influences R5 HIV-1 replication, including late stages of the viral lifecycle. To evaluate the effect of V3 loop on viral replication with respect to CCR5 expression, 45 replication-competent mutant viruses carrying multiple amino acid substitutions in the gp120 V3 loop were used which were derived from an R5 HIV-1 V3 loop library using HIV-$1_{JR\text{-}FLan}$ as background (34). The library contained a set of random combinations of 0–10 polymorphic amino acid substitutions observed in 31 R5 clinical isolates. Replication of the viruses in a CD4 T-cell line PM1 expressing low levels of CCR5 and PM1/CCR5 cells expressing

* This work was supported by grants from the Ministry of Education, Science, Sports, and Culture and the Ministry of Health Labor and Welfare, Japan, and in part by the Cooperative Research Project on Clinical and Epidemiological Studies of Emerging and Re-emerging Infectious (Renkei Jigyo: no. 78, Kumamoto University). The costs of publication of this article were defrayed in part by the payment of page charges. This article must therefore be hereby marked "*advertisement*" in accordance with 18 U.S.C. Section 1734 solely to indicate this fact.

[1] To whom correspondence should be addressed. Tel.: 81-96-373-5130; Fax: 81-96-373-5132; E-mail: yusak@kumamoto-u.ac.jp.

[2] The abbreviations used are: HIV, human immunodeficiency virus; mAb, monoclonal antibodies; PBS, phosphate-buffered saline; ELISA, enzyme-linked immunosorbent assay.

high levels of CCR5 was examined. It was found that the viruses revealed different replication phenotypes with respect to CCR5 expression. The present study focused on a viral clone, HIV-$1_{V3L\#08}$, with a replication in PM1 cells comparable with wild type HIV-$1_{JR\text{-}FLan}$ but with dramatically suppressed replication in PM1/CCR5 cells. This is the first report that suppression of replication by high expression of CCR5 is V3 loop-dependent and associated with late stages of viral replication.

EXPERIMENTAL PROCEDURES

Cells and Viruses—The human CD4 T-cell line PM1 (35) was provided by the National Institutes of Health (NIH) AIDS Research and Preference Reagent Program, Division of AIDS NIAID, NIH, and maintained in RPMI1640 (Invitrogen) supplemented with 10% heat-inactivated fetal calf serum (Vitromex). PM1/CCR5 cells were generated by standard retrovirus-mediated transduction of PM1 cells by coculture with PA317 clone #8 cells transfected with pG1TKneo-CCR5 (36) without cloning. MAGIC5 (37) and 293T cells were maintained in Dulbecco's modified Eagle's medium (ICN Biomedicals) supplemented with 10% heat-inactivated fetal calf serum.

pJR-FL_{an} was created in our laboratory from pJR-FL (kindly provided by Dr. Y. Koyanagi, Kyoto University), incorporating AflII and NheI sites into Env at 6395 and 6562 nucleotides, respectively. R5 viruses, carrying a set of random amino acid substitutions in the gp120 V3 loop, were derived from the HIV-1 V3 loop library (34). For construction of V3 loop mutant viruses, amino acid substitutions were introduced into the gp120 V3 loop of pJR-FL_{an}, as described previously (34). For virus preparation, 293T cells (1 10^6) were transfected with 10 g of molecular clone DNA using the calcium phosphate ProFection Mammalian Transfection System (Promega). The supernatant was collected at 28 h post-transfection and filtered through a 0.22- m filter unit (Millipore) and stored at 80 °C until use.

HIV-1 single-cycle luciferase reporter viruses were produced by cotransfection of 293T cells with pNL-LucR E (38) and Env-expressing plasmids pCXN-$Env_{JR\text{-}FLan}$, pCXN-$Env_{JR\text{-}FLan\text{-}A69T}$, pCXN-$Env_{V3L\#08}$, or pCXN-$Env_{V3L\#08\text{-}A69T}$. Culture supernatant containing pseudoviruses at a final concentration of 8 ng/ml p24 was added to 1 10^4 cells/well PM1 or PM1/CCR5 cells in a 48-well plate. After 2 h, the cells were washed twice with phosphate-buffered saline (PBS), and firefly luciferase activity was measured 48 h post-infection according to the manufacturer's directions (Promega).

Viral Replication Assay—For determination of replication phenotype, 4 10^4 of PM1 or PM1/CCR5 cells were infected with 8 ng of p24 Gag for 2 h. After washing twice with PBS, the infected cells were incubated at 37 °C in a 5% CO_2 atmosphere. On day 6 post-infection, p24 Gag in the supernatant was measured using a p24 Gag ELISA (Zeptometrix).

Flow Cytometry—Cell surface expression of CD4 and CCR5 was analyzed by flow cytometry. Cells were incubated in the staining solution (3% fetal calf serum plus 0.05% sodium azide in PBS) with the mouse monoclonal antibodies (mAbs) anti-human CD4 (SK3, BD Biosciences Pharmingen) or anti-human CCR5 (2D7, BD Biosciences Pharmingen) at 4 °C for 30 min. The cells were washed with PBS, and fluorescein isothiocyanate-conjugated goat anti-mouse IgG antibody was used for antibody-staining. Flow cytometry was performed with a FACSCalibur flow cytometer (BD Biosciences) and analyzed with BD Cell Quest Version 3.1 software (BD Biosciences Pharmingen).

Quantitative PCR—Virus (8 ng p24 Gag) was pretreated in culture fluids with 690 units of DNase I (Worthington Biochem) and added to PM1 or PM1/CCR5 cells (4 10^4) for 2 h at 37 °C. Cells were then washed and incubated at 37 °C for 8 h. Total DNA was purified using the QIAamp DNA blood kit (Qiagen) and eluted in a total volume of 200 l. Two l of DNA was analyzed by real-time quantitative PCR. Late reverse transcription products were detected using primers amplifying the region between nucleotides 685 and 789 of the provirus: forward primer (5 -ACATCAAGCAGCCATGCAAAT-3), reverse primer (5 -ATCTGGCCTGGTGCAATAGG-3), and probe (5 -FAM-CATCAATGAGGAAGCTGCAGAATGG-GATAGA-TAMRA-3). Reactions were performed in triplicate in TaqMan Universal PCR master mix using 0.9 pmol of each primer/ l and 0.25 pmol of probe/ l. After 10 min at 95 °C, reactions were cycled for 15 s at 95 °C followed by 1 min at 60 °C for 40 repeats on an ABI Prism model 7700 thermal cycler (Applied Biosystems).

Virus Infectivity Assay—For infectivity assay, 5 10^3 of MAGIC5 cells (37) were plated 1 day before infection into 48-well tissue culture plates. After absorption of virus for 2 h at 37 °C, cells were washed twice with PBS and further incubated at 37 °C in 5% CO_2. At 48 h post-infection, the cells were stained, and the number of blue foci in each well was counted (39).

Western Blot Analysis—Four days post-infection, viruses in the supernatant of HIV-1-infected cells were pelleted by centrifugation at 175,000 *g* for 60 min. Viral proteins (10 ng of p24 Gag) were separated by 4–20% SDS-PAGE, transferred to a polyvinylidene difluoride Immobilon P membrane (Millipore), and blocked with 5% milk in PBST (137 mM NaCl, 8.1 mM Na_2HPO_4, 2.68 mM KCl, 1.47 mM KH_2PO_4, and 0.05% Tween 20) for 8 h at room temperature. Immunodetection was performed with anti-gp120 antibody (Aalto Bio Reagents) and anti-gp41 antibody (2F5; National Institutes of Health AIDS Research and Preference Regent Program) followed by a secondary antibody conjugated to horseradish peroxidase (Sigma) and Chemi-Lumi One (Nacalai Tesque).

Virus Precipitation Assay—Virus immunoprecipitation assay was performed as described previously (40). Anti-HLA-DR (L243), anti-CCR5 (3A9), and anti-CXCR4 (12G5) mAbs were purchased from BD Biosciences Pharmingen. Anti-CCR5 (T21/8) mAb was purchased from BioLegend. A rat immunoglobulin G1 (IgG1) mAb against hepatitis C virus, Mo-8 (41), was used as a rat isotype-matched negative control. Virus (5 ng of p24 Gag) in PBS containing 3% bovine serum albumin was mixed with the mAb at a concentration of 10 g/ml in a final volume of 100 l and incubated for 12 h at 4 °C. Then, 10 l of Pansorbin (Calbiochem), a suspension of heat-killed *Staphylococcus aureus* cells pretreated for 1 h with 3% bovine serum albumin, was added to the virus/mAb mixture. After incubation for 30 min at room temperature, captured viruses were

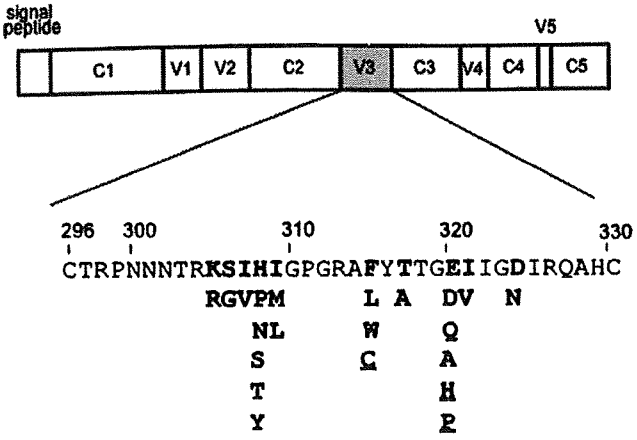

FIGURE 1. **Amino acid substitutions of the R5 HIV-1 V3 loop library.** Each viral clone contained 0–10 substitutions in the gp120 V3 loop. pJR-FL_{an} was used to construct the library as background. Theoretically, the number of possible combinations of 0–10 amino acid substitutions was calculated as 27,648. Residues in *boldface* indicate the substitutions that were randomly incorporated. *Underlined* residues indicate the substitutions that were not detected in the 31 R5 viruses, Phe^{315} to Cys or Glu^{320} to His or Pro but inevitably incorporated into the library due to combinations of nucleotide substitutions.

removed by centrifugation (350 *g* for 30 min). p24 Gag in the supernatant was determined by p24 Gag ELISA.

RESULTS

Replication Suppression of Viruses from the R5 HIV-1 V3 Loop Library in PM1/CCR5 Cells—An R5 HIV-1 V3 loop library was constructed carrying a set of random combinations of 0–10 amino acid substitutions in the V3 loop (34) (Fig. 1). Replication of 45 viruses randomly selected from the library was compared in PM1 and PM1/CCR5 cells (Table 1). PM1/CCR5 cells, generated by standard retrovirus transduction of PM1 cells with a CCR5 expression lentivector, regularly expressed high level of CCR5 and with similar levels of CD4 compared with PM1 cells (Fig. 2). A total of 36% of the viruses (16/45) failed to replicate in both cell types (1.0 ng/ml p24 Gag on day 6). Among replication competent viruses, ratios of p24 Gag ranged from 0.1 to 27, whereas the parental virus, $HIV\text{-}1_{JR\text{-}FLan}$, could replicate in both PM1 and PM1/CCR5 cells (ratio 1.9). Viruses were classified into the following three groups; 1) those that grew 10-fold more in PM1/CCR5 than PM1 cells (ratio 10), designated $R5^{H}$ phenotype, 2) those that revealed comparative replication kinetics in PM1 and PM1/CCR5 cells (0.1 ratio 10), designated $R5^{HL}$, and 3) viruses where replication was drastically suppressed in PM1/CCR5 cells (ratio 0.1), designated $R5^{L}$. Six of 45 viruses (13%), including $HIV\text{-}1_{V3L\#10}$, $HIV\text{-}1_{V3L\#16}$, $HIV\text{-}1_{V3L\#21}$, $HIV\text{-}1_{V3L\#23}$, $HIV\text{-}1_{V3L\#29}$, and $HIV\text{-}1_{V3L\#34}$, were classified as $R5^{H}$ phenotype, whereas 3 of the 45 (6.7%) viral clones, $HIV\text{-}1_{V3L\#08}$, $HIV\text{-}1_{V3L\#23}$, and $HIV\text{-}1_{V3L\#25}$, were $R5^{L}$ phenotype. These results indicated that the R5 HIV-1 V3 loop library contained unique replication phenotypes with respect to expression levels of CCR5 in the CD4 T-cell line. Note that these viruses carried amino acid substitutions in the V3 loop alone, indicating that the variety of replication phenotypes was dependent on their V3 loop structure.

Attention was then focused on the $R5^{L}$ phenotype, $HIV\text{-}1_{V3L\#08}$, to ascertain why high expression of CCR5 had a suppressive effect on viral replication. Replication of $HIV\text{-}1_{V3L\#08}$ was markedly suppressed in PM1/CCR5 cells, whereas the virus showed similar replication kinetics to $HIV\text{-}1_{JR\text{-}FLan}$ with 8 ng of p24 Gag in PM1 cells (Fig. 3, *A* and *B*). On day 6 post-infection, p24 Gag in the supernatant was 33-fold lower in PM1/CCR5 than PM1 cells. However, no replication suppression of $HIV\text{-}1_{V3L\#08}$ was observed in peripheral blood mononuclear cells or macrophages derived from three different donors compared with $HIV\text{-}1_{JR\text{-}FLan}$ (data not shown). $HIV\text{-}1_{V3L\#08}$ contained 8 amino acid substitutions: Ile^{307} to Val, His^{308} to Thr, Ile^{309} to Met, Phe^{315} to Leu, Thr^{317} to Ala, Glu^{320} to Asp, Ile^{321} to Val, and Asp^{324} to Asn in gp120 V3 loop alone (Fig. 3*C*).

A revertant of $HIV\text{-}1_{V3L\#08}$, designated $HIV\text{-}1_{V3L\#08\text{-}A69T}$, was isolated that restored replication ability in PM1/CCR5 cells with an additional substitution Ala^{69} to Thr in the C1 region of gp120 (Fig. 3*C*). $HIV\text{-}1_{JR\text{-}FLan\text{-}A69T}$ and $HIV\text{-}1_{V3L\#08\text{-}A69T}$ showed similar replication kinetics to $HIV\text{-}1_{JR\text{-}FLan}$ in PM1 cells (Fig. 3*A*). However, $HIV\text{-}1_{JR\text{-}FLan\text{-}A69T}$ and $HIV\text{-}1_{V3L\#08\text{-}A69T}$ showed a slightly higher replication profile in PM1/CCR5 cells on days 4 and 5 compared with $HIV\text{-}1_{JR\text{-}FLan}$ (Fig. 3*B*).

It is possible that suppression of $HIV\text{-}1_{V3L\#08}$ replication in PM1/CCR5 cells was due to high susceptibility of the virus to the chemokine(s) produced by the cells. To exclude this possibility, susceptibility of $HIV\text{-}1_{V3L\#08}$, $HIV\text{-}1_{V3L\#08\text{-}A69T}$, $HIV\text{-}1_{JR\text{-}FLan}$, and $HIV\text{-}1_{JR\text{-}FLan\text{-}A69T}$ to a -chemokine, RANTES (regulated on activation normal T cell expressed and secreted), was measured, but no differences were detected (data not shown).

Entry Efficiency of $HIV\text{-}1_{V3L\#08}$ into PM1/CCR5 Cells—To investigate whether the entry efficiency of $HIV\text{-}1_{V3L\#08}$ decreased, real-time PCR was utilized to analyze cellular accumulation of the late reverse transcriptase product, *gag*, synthesized shortly after virus entry into the cells (Fig. 4*A*). There was no decrease in *gag* DNA synthesis of $HIV\text{-}1_{V3L\#08}$ in PM1/CCR5 compared with PM1 cells. Rather, the DNA copies of $HIV\text{-}1_{V3L\#08}$ were 3.3-fold higher in PM1/CCR5 than in PM1 cells. Higher expression of CCR5 could promote more efficient viral entry when CD4 is not significantly expressed, consistent with previous reports for other viruses (1.9–2.5-fold) (6, 8). Moreover, there was no clear difference in DNA synthesis among the four viruses in PM1/CCR5 cells.

In addition, the virus pseudotyped with the envelope proteins of $HIV\text{-}1_{V3L\#08}$ revealed 2.0-fold more efficiency in PM1/CCR5 than in PM1 cells (Fig. 4*B*). Luciferase activity of other viruses in PM1/CCR5 cells also increased 1.7–2.2-fold compared with PM1 cells. Measured luciferase activity in cells infected with pseudotyped viruses serves as an indirect estimation of viral entry, integration, and transcriptional activity. The results demonstrate that suppression of $HIV\text{-}1_{V3L\#08}$ replication in PM1/CCR5 cells is not associated with early stages of the viral lifecycle.

Production of Virus from PM1/CCR5 Cells Infected with $HIV\text{-}1_{V3L\#08}$—A comparison was made of the number of virions generated from PM1/CCR5 and PM1 cells in the presence of a reverse transcriptase inhibitor (AZT) and a CCR5 inhibitor